phys. stat. sol. (c) **1**, No. 4, 706–709 (2004) / **DOI** 10.1002/pssc.200304298

# Determination and modeling of the optical constants of direct band gap $Be_xZn_{1-x}Te$ grown by molecular beam epitaxy

**M. Muñoz**[*, 1], **O. Maksimov**[2], **M. C. Tamargo**[1], **M. R. Buckley**[3], and **F. C. Peiris**[3]

[1] Department of Chemistry, The City College of New York, New York, NY 10031, USA
[2] Department of Physics, Pennsylvania State University, University Park, PA 16802, USA
[3] Department of Physics, Kenyon College, Gambier, Ohio 43022, USA

Received 1 October 2003, revised 2 December 2003, accepted 4 December 2003
Published online 18 February 2004

**PACS** 78.20.Ci

The optical constants $\varepsilon(E)$ of direct band gap $Be_xZn_{1-x}Te$ have been measured at 300 K using spectral ellipsometry (0.73–6.45 eV). The $\varepsilon(E)$ spectra displayed distinct structures associated with critical points at $E_0$, $E_0+\Delta_0$, $E_1$, $E_1+\Delta_1$, $e_1+\Delta_1$ and $E_2$. The experimental data over the entire measured spectral range has been fit using the Holden-Muñoz model dielectric function, which is based on the electronic energy-band structure near critical points plus excitonic and band-to-band Coulomb-enhancement effects at $E_0$, $E_0+\Delta_0$ and the $E_1$, $E_1+\Delta_1$, doublet. In addition to evaluate the energies of these various band-to-band critical points, information about the binding energy ($R_1$) of the two-dimensional exciton related to the $E_1$, $E_1+\Delta_1$ critical points was obtained. The value of $R_1$ was in good agreement with effective mass theory. The ability to evaluate $R_1$ has important ramifications for first-principles band-structure calculations that include exciton effects at $E_0$, $E_1$, and $E_2$.



**1 Introduction** II–VI semiconductor optoelectronic devices based on beryllium are currently under investigation in order to overcome important problems such as low *p*-type doping carrier concentration and degradation issues present in several II–VI devices. In order to design efficient optoelectronic devices involving these compounds a detailed study of the optical constants of $Be_xZn_{1-x}Te$ as well as its relation with their band structure is necessary. However, in spite of its fundamental and applied significance, relatively little work has been reported on the optical properties related to the electronic band. Some authors [1] performed measurements of the ZnTe dielectric function but modeled the optical constants not including continuum exciton contributions, i.e., band-to-band Coulomb enhancement (BBCE) effects at $E_0$, $E_0+\Delta_0$, $E_1$, $E_1+\Delta_1$ critical points (CPs). References [2] and [3] using Fourier analysis and a second derivative analysis of the dielectric function, respectively, were able to obtain the energies of features related to the CPs. Reference [3], using a second derivative analysis of the dielectric, function provided the only study available of the energies of features related to the CPs of $Be_xZn_{1-x}Te$ for $x > 0$. In this work we present a study of the optical constants of direct band gap $Be_xZn_{1-x}Te$ and their relationship with their band structure. The $\varepsilon(E)$ spectra of the different samples displayed distinct structures associated with CPs at $E_0$, $E_0+\Delta_0$ $E_1$, $E_1+\Delta_1$, the $e_1+\Delta_1$ feature, as well as $E_2$. The experimental data over the entire measured spectral range has been fit using the Holden-Muñoz model [4] dielectric function, which is based on the electronic energy-band structure near the CPs plus excitonic and BBCE effects. In addition to evaluating the energies of these various band-to-band CPs, information about the binding energy ($R_1$) of the two-dimensional exciton related to the $E_1$ and $E_1+\Delta_1$ CPs was obtained. The value of $R_1$ was

[*] Corresponding author: e-mail: mmunoz@sci.ccny.cuny.edu, Phone: +1 212 6508376, Fax: +1 212 6506848

in good agreement with effective mass/$\boldsymbol{k}\cdot\boldsymbol{p}$ theory [5]. The ability to evaluate $R_1$ has important ramifications for first-principles band-structure calculations that include exciton effects at $E_0$, $E_1$, and $E_2$ [6].

**2 Experimental details** The films were grown by molecular beam epitaxy (MBE) on semi-insulating epiready (001) InP substrates using a Riber 2300 MBE system. The substrates were deoxidized at 500 °C under As flux, and a ~100 nm-thick, lattice matched InGaAs buffer layer was grown on the InP substrate. The growth temperature for the $Be_xZn_{1-x}Te$ layer was maintained at 270 °C. The growth rate was approximately 0.5 μm/h, and $Be_xZn_{1-x}Te$ layers were 0.5–1.5 μm thick. The compositions of the $Be_xZn_{1-x}Te$ samples for this study, $x$ = 0, 0.03, 0.09 and 0.19, were determined using single-crystal x-ray diffraction. The determination of the dielectric function was done by spectroscopic ellipsometry (SE), the details of these measurements as well as the analysis performed are described in Ref. [3].

**3 Model, results and discussion** Shown by solid lines in Fig. 1 (a) are the experimental values of the real and imaginary components of the dielectric function for $Zn_{0.97}Be_{0.03}Te$, as function of the photon energy, similar lineshapes were observed for the other compositions. In the direct-gap zincblende-type semiconductor $Be_xZn_{1-x}Te$ ($x < 0.28$) [7] the spin-orbit interaction splits the highest-lying $\Gamma_{15}^{v}$ valence band into $\Gamma_8^v$ and $\Gamma_7^v$ (splitting energy $\Delta_0$ ). The corresponding lowest-lying transitions at $k$ = 0 [three-dimensional (3D) $M_0$] are labeled $E_0$ [ $\Gamma_8^v - \Gamma_6^c$ ] and $E_0+\Delta_0$ [ $\Gamma_7^v - \Gamma_6^c$ ], respectively. The corresponding 2D $M_0$ CPs are designated $E_1$ [ $L_{4,5}^v - L_6^c$ or $\Lambda_{4,5}^v - \Lambda_6^c$ ] and $E_1+\Delta_1$ [ $L_6^v - L_6^c$ or $\Lambda_6^v - \Lambda_6^c$ ], respectively. The $e_1+\Delta_1$, feature corresponds to a $L_3$–$L_1$ transition. The $E_2$ feature is due to transitions along ⟨110⟩ (Σ) or near the X point.

The experimental data over the entire measured spectral range has been fit using the Holden-Muñoz model [4] dielectric function which is based on the electronic energy-band structure near these CPs plus excitonic and BBCE effects at $E_0$, $E_0+\Delta_0$, and the $E_1$, $E_1+\Delta_1$, doublet. The data near the $E_0$ band gap were fit to a function which contains Lorentzian-broadened (a) discrete excitonic (DE) and (b) 3D $M_0$ BBCE contributions. References [8] and [9] have demonstrated that even if the $E_0$ exciton is not resolved, the Coulomb interaction still affects the band-to-band line shape. Thus, $\varepsilon_2(E)$ is given by [4]

$$\varepsilon_{2,E_0}(E) = \mathrm{Im}\left\{\frac{A}{E^2}\left[2R_0\left(\frac{1}{(E_0-R_0)-E-i\Gamma_0^{ex}}+\frac{1}{(E_0-R_0)+E+i\Gamma_0^{ex}}\right)+\int_{-\infty}^{\infty}\left(\frac{\theta(E'-E_0)}{1-e^{-2\pi\, z_1(E')}}-\frac{\theta(-E'-E_0)}{1-e^{-2\pi\, z_2(E')}}\right)\frac{dE'}{E'-E_0-i\Gamma_0}\right]\right\}, \tag{1}$$

where $A$ is a constant, $E_0$ is the energy of the direct gap, $R_0$ is the effective Rydberg energy, $\Gamma_0^{ex}$ is the broadening parameter of the first state of the exciton, $\Gamma_0$ is the broadening parameter for the band-to-band transition, $z_1(E) = \sqrt{R_0/(E-E_0)}$ , $z_2(E) = \sqrt{R_0/(-E-E_0)}$ and $\theta(x)$ is the unit step function. The terms in parentheses and under the integral in Eq. (1) correspond to the DE and BBCE contributions, respectively. Since the DE was not resolved, we took $\Gamma_0^{ex} = \Gamma_0$ . The $E_0+\Delta_0$ transition has also been described by a function similar to Eq. (1), i.e., $\tilde{\varepsilon}_{E_0}(E) \to \tilde{\varepsilon}_{E_0+\Delta_0}(E), A \to B$, $E_0 \to E_0+\Delta_0$, $R_0 \to R_{so}$, $\Gamma_0^{ex} \to \Gamma_{so}^{ex}$, and $\Gamma_0 \to \Gamma_{so}$ . For the $E_1$ and $E_1+\Delta_1$ CPs, $\varepsilon_2(E)$ is written using an equation [4] equivalent to equation (1), containing the discrete exciton plus the BBCE contributions. For the $E_1$ and $E_1+\Delta_1$ CPs the model parameters are $C_1$, $E_1$, $R_1$, $\Gamma_1^{ex}$, $\Gamma_1$, and $C_2$, $E_1+\Delta_1$, $R_{1so}$, $\Gamma_{so}^{ex}$, $\Gamma_{1so}$, respectively. The nature of $e_1+\Delta_1$ and $E_2$ features is more complicated in relation to $E_0$, $E_0+\Delta_0$ and $E_1$, $E_1+\Delta_1$ since they do not correspond to a single, well-defined CP. Therefore, each was described by a damped harmonic oscillator term [4] with an amplitude F and broadening parameter $\gamma$. A constant $\varepsilon_{1\infty}$ was added to the real part of the dielectric constant to account for the vacuum plus contributions from higher-lying energy gaps ( $E_0'$, etc.). This quantity should not be confused with the high frequency dielectric constant $\varepsilon(\infty)$. In order to reduce the contributions of $E_1$ to $\varepsilon_2(E)$ below the fundamental gap $E_0$ we have introduced a linear cut-off for $\varepsilon_2(E)$, obtaining the corrected imaginary dielectric $\varepsilon_{2,\mathrm{co}}$:

$$\varepsilon_{2,co}(E) = \varepsilon_2(E)\frac{E-E_0}{E_{co}-E_0} \ , \tag{2}$$

where $E_{co}$ is the cutoff energy and $E_0$ is the direct bandgap. $\varepsilon_1$ was corrected by a numerical Kramers-Kronig (KK) analysis of Eq. (2). In order to calculate $R_1$ using the $\boldsymbol{k}\cdot\boldsymbol{p}$ theory we follow the procedure provided in Ref. [4], with the high frequency dielectric constant $\varepsilon(\infty) = 7.28$ and the matrix element $E_p = 23$ eV [7]. The results of this calculation are $R_1 = 244$, 253, 256, and 261 meV for beryllium compositions $x = 0$, 0.03, 0.10, and 0.19, respectively. Table 1 summarizes the results of our fit.

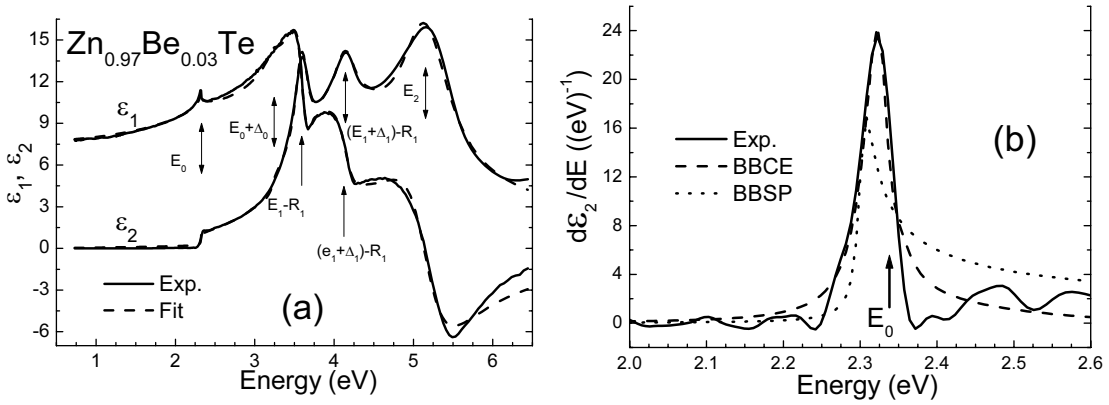


**Fig. 1** (a) Solid and dashed lines are the experimental and fit values, respectively, of the dielectric function $\varepsilon$ for $Zn_{0.97}Be_{0.03}Te$ (b) $\varepsilon_2$ numerical derivative of the experimental data, fit using BBCE lineshape and parabolic one, respectively.

The dielectric function spectra determined for ZnTe is in agreement with prior studies of this material [1, 2]. The optical constants $\varepsilon_1$ and $\varepsilon_2$ for ZnTe over an extended range, have been investigated by a number of authors [1], using SE, however, they used a model in which the $E_0$ CP is represented by only Lorenztian broadened band-to-band single-particle (BBSP) expressions, i.e., no DE. As mentioned above the optical structure associated with the $E_1$ CP is primarily excitonic. Reference 1 did not include the BBCE contribution neither at $E_0$ nor $E_1$. Excitonic effects at the $E_0$ CP also must be included, even at room temperature, in the presence of a DE, the band-to-band $E_0$ lineshape (within about 6–10 $R_0$) is changed from the BBSP square root (broadened) term to a three-dimensional BBCE expression, which has a lineshape similar to a step function (broadened), as shown in Fig. 1(a), and also increases the amplitude of the absorption in relation to the BBSP expression [4]. The inadequacy of the BBSP approach at $E_0$ is clearly demonstrated in Fig. 1(b), where the dotted line is a fit of the $E_0$ feature to the first derivative of a 3D $M_0$ BBSP expression. Note that the fit is quite asymmetric on the high-energy side, while the experimental curve is symmetric, consistent with a BBCE line shape. Thus, Fig. 1(b) demonstrates conclusively that even if the exciton is not resolved the lineshape is BBCE and not BBSP, in agreement with Refs. [8] and [9].

The ability to measure $R_1$ has considerable implications for band-structure calculations, both empirical and first principles [6, 10]. In the former case, band-structure parameters, e.g., pseudopotential form factors, are determined mainly by comparison with optical and modulated optical experiments, including the "$E_1$, $E_1+\Delta_1$" features. Therefore, the band-to-band energies are too low by an amount $R_1$. Rohlfing and Louie have published a first-principles calculation of the optical constants of GaAs, including excitonic effects [6]. Using this formalism they have also calculated $R_0$. Their approach also makes it possible to evaluate $R_1$ from first-principles [11]. Albrecht et al. [10] also have presented an ab initio approach for the calculation of excitonic effects in the optical spectra of semiconductors and insulators. However, to date they have presented results for only Si. The consideration of the excitonic effects at $E_0$, $E_0+\Delta_0$, $E_1$ and $E_1+\Delta_1$ during the modeling of the dielectric function is a fundamental consideration as discussed in Ref. [4].

In summary, we have measured the room-temperature complex dielectric function of direct band gap $Be_xZn_{1-x}Te$ in the range of 0.73–6.45 eV using SE. The experimental data over the entire measured spectral range has been fit using the Holden-Muñoz model for the dielectric function, which is based on the electronic energy-band structure near these CPs plus DE and BBCE effects at $E_0$, $E_0+\Delta_0$, $E_1$, and $E_1+\Delta_1$. In addition to determining the energy of $E_0$ CP, using the effective mass/$\boldsymbol{k\cdot p}$ theory we have evaluated the 2D exciton binding energy $R_1$ (= 214 meV). The line shape of the imaginary part of $Be_xZn_{1-x}Te$ dielectric function and its derivative demonstrates clearly that excitonic effects, even at room temperature and with no exciton resolved, must be taken into account using a BBCE line shape and not a BBSP.

**Table 1** Values of the relevant parameters obtained in this experiment for $Be_xZn_{1-x}Te$.

| Parameter/ Sample | $A$ ($eV^{1.5}$) | $E_0$ (eV) | $\Gamma_0$ (meV) | $B$ ($eV^{1.5}$) | $E_0+\Delta_0$ (eV) | $\Gamma_{so}$ (meV) | $C_1$ ($eV^2$) | $E_1-R_1$ (eV) | $\Gamma_1$ (meV) | $R_1$ (meV) |
|---|---|---|---|---|---|---|---|---|---|---|
| ZnTe | 1.30 | 2.289 | 40 | 5.18 | 3.22 | 66 | 10.51 | 3.580 | 89 | 217 |
| $Zn_{0.97}Be_{0.03}Te$ | 1.55 | 2.340 | 6 | 5.98 | 3.25 | 42 | 10.96 | 3.595 | 99 | 213 |
| $Zn_{0.90}Be_{0.10}Te$ | 1.60 | 2.435 | 8 | 6.00 | 3.30 | 63 | 11.00 | 3.614 | 120 | 213 |
| $Zn_{0.81}Be_{0.19}Te$ | 2.85 | 2.72 | 16 | 6.00 | 3.319 | 80 | 8.04 | 3.714 | 96 | 214 |

| Parameter/ Sample | $C_2$ ($eV^2$) | $E_1+\Delta_1-R_1$ (eV) | $\Gamma_1^{so}$ (meV) | $E_{co}$ (eV) | $F_1$ (eV) | $e_1+\Delta_1$ (eV) | $\gamma_1$ (meV) | $F_2$ (eV) | $E_2$ (eV) | $\gamma_2$ (meV) |
|---|---|---|---|---|---|---|---|---|---|---|
| ZnTe | 14.31 | 4.139 | 147 | 3.04 | 1.17 | 3.980 | 264 | 1.90 | 5.144 | 153 |
| $Zn_{0.97}Be_{0.03}Te$ | 13.53 | 4.147 | 165 | 2.97 | 1.22 | 4.130 | 323 | 1.50 | 5.160 | 144 |
| $Zn_{0.90}Be_{0.10}Te$ | 15.00 | 4.187 | 193 | 2.72 | 1.50 | 4.015 | 340 | 1.3 | 5.152 | 153 |
| $Zn_{0.81}Be_{0.19}Te$ | 12.03 | 4.286 | 164 | 3.46 | 0.91 | 4.059 | 205 | 2.17 | 5.13 | 205 |

**Acknowledgements** This work was supported by the National Science Foundation through grant number ECS0217646. Partial support was also obtained from the Center for Analysis of Structures and Interfaces, and the New York State Center for Advanced Technology on Photonic Materials and Applications.

## References

[1] K. Sato and S. Adachi, J. Appl. Phys. **73**, 926 (1993);
K. Suzuki and S. Adachi, J. Appl. Phys. **82**, 1320 (1997).
[2] Y. D. Kim, S. G. Choi, M. V. Klein, S. D. Yoo, D. E. Aspnes, S. H. Xin, and J. K. Furdyna, Appl. Phys. Lett. **70**, 610 (1997).
[3] M. R. Buckley, F. C. Peiris, O. Maksimov, M. Muñoz, and M. C. Tamargo, Appl. Phys. Lett. **70**, 5156 (2002).
[4] M. Muñoz, T. M. Holden, F. H. Pollak, M. Kahn, D. Ritter, L. Kronik, and G. M. Cohen, J. Appl. Phys. **92**, 5878 (2002).
[5] Y. Petroff and M. Balkanski, Phys. Rev. B **3**, 3299 (1971);
E. O. Kane, Phys. Rev. **180**, 852 (1969).
[6] M. Rohlfing and S. G. Louie, Phys. Rev. Lett. **81**, 2312 (1998).
[7] M. Cardona and D. L. Greenaway, Phys. Rev. **131**, 98 (1963).
[8] M. Muñoz, Y. S. Huang, F. H. Pollak, and H. Yang, J. Appl. Phys. **93**, 2549 (2003).
[9] F. H. Pollak, M. Muñoz, T. Holden, K. Wei, and V. M. Asnin, phys. stat. sol. (b) **215**, 33 (1999).
[10] S. Albrecht, L. Reining, R. Del Sole, and G. Onida, Phys. Rev. Lett. **80**, 4510 (1998).
[11] Louie (private communication).